Chaos, Solitons and Fractals 189 (2024) 115672

Contents lists available at ScienceDirect

Chaos, Solitons and Fractals

journal homepage: www.elsevier.com/locate/chaos

Azimuthally dependent spontaneous emission from a coherently microwave-field driven four-level atom-light coupling scheme

Muqaddar Abbas [a], Seyyed Hossein Asadpour [b], Rahmatullah [c], Feiran Wang [d,*], Hamid R. Hamedi [e,*], Pei Zhang [a,*]

[a] Ministry of Education Key Laboratory for Nonequilibrium Synthesis and Modulation of Condensed Matter, Shaanxi Province Key Laboratory of Quantum Information and Quantum Optoelectronic Devices, School of Physics, Xi'an Jiaotong University, Xi'an 710049, China
[b] School of Physics, Institute for Research in Fundamental Sciences, IPM, Tehran, 19395-5531, Iran
[c] Quantum optics Lab. Department of Physics, COMSATS University Islamabad, Islamabad, Pakistan
[d] School of Science of Xi'an Polytechnic University, Xi'an 710048, China
[e] Institute of Theoretical Physics and Astronomy, Vilnius University, Sauletekio 3, Vilnius 10257, Lithuania

ARTICLE INFO

Keywords:
Orbital angular moment
Spontaneous emission
Superradiance
Quantum information processing

ABSTRACT

We present a novel technique that makes use of vortex light beams for generating spatially structured spontaneously emission in a atomic four-level configuration. This atomic configuration consists of two closely spaced excited levels linked to a microwave field and two optical vortex fields connecting them to the ground state. After that, the excited states eventually decays to a fourth metastable level. We find that spatially dependent spontaneous emission spectra may be obtained by efficiently transferring the orbital angular momentum (OAM) of the vortex-pumping light beams to the spontaneously emitted photons. This enables the targeted quenching of spontaneous emission in specific azimuthal regions, while simultaneously enhancing it in others. By effectively controlling the OAM of optical vortices and taking into account the correlations of the atomic gas and their collective decay to a metastable state via superradiance, it might be feasible to experimentally modify the probabilistic emission process with deterministic radiation. The approach we propose might be helpful in controlling the quantum level emission characteristics via the nonlinear interaction of the atom–vortex-beam light.

1. Introduction

The exploration of coherent control over the optical properties of a medium has emerged as a focal point of considerable interest. Within this domain, the interplay of coherence and interference stands out as a crucial research theme in the field of quantum optics [1]. Quantum interference, a key player in this scenario, introduces substantial variations in the way a system responds to an applied optical field, notably allowing for the modulation of atomic spontaneous emission through the influence of control fields [2–4]. Spontaneous emission occurs as a consequence of the interaction between atoms and environmental modes in an atomic system. Diverse methods have been devised to control and shape the spontaneous emission spectrum [2–4], opening avenues to explore various optical phenomena. These phenomena encompass laser emission without population inversion [5], electromagnetic transparency [6], correlated spontaneous emitters [7], and enhancing with zero absorption refractive index [8].

In the intricate landscape of atomic multilevel systems, modifications in spontaneous emission become conceivable through both passive and active measures. Passive control, exemplified by the placement of atoms in reservoir density modes distinct from vacuum modes [9], finds application in micro-cavities [10] and micro-resonators with atoms or materials possessing a photonic band gap [11]. Active control, on the other hand, relies on external factors, including radio-frequency microwave, optical, and other fields [12]. Coherent light beams present a viable avenue for controlling spontaneous emission by adjusting the intensity or frequency of the laser field [13]. Moreover, spontaneous emission spectra can be molded through phase control and other innovative approaches. Proposals, such as modulating spontaneous emission spectra through phase-dependent effects by designing atoms along with control fields system have been put forth [2]. Investigations have also delved into the manipulation of spontaneous emission by considering a four-level atom driven by two lasers with the same frequency [14].

* Corresponding authors.
E-mail addresses: feiran0325@xjtu.edu.cn (F. Wang), hamid.hamedi@tfai.vu.lt (H.R. Hamedi), zhangpei@mail.ustc.edu.cn (P. Zhang).

https://doi.org/10.1016/j.chaos.2024.115672
Received 29 May 2024; Received in revised form 26 September 2024; Accepted 15 October 2024
Available online 30 October 2024

Notably, the relative phase of the pump fields in this setup has demonstrated the potential for achieving complete suppression of spontaneous emission, marking a significant stride in the precise control of quantum optics phenomena.

Light, a carrier of both energy and momentum, undergoes momentum exchange when engaging with matter and an optical field. Momentum, comprised of angular and linear components, further breaks down into orbital and spin parts. The orbital segment is associated with the transverse angular phase of light, expressed as $e^{il\Phi}$—recognized as OAM. Conversely, the spin component aligns with polarization. Notably, Gaussian modes, including Laguerre–Gaussian (LG) mode light, have been shown to accommodate finite OAM [15]. The past two decades have witnessed heightened interest in LG mode light, driven by its distinctive attributes. The presence of nonzero OAM introduces a captivating element to the intensity profile, where the strength of beam's diminishes at its central point in the direction that is transverse, resulting in a characteristic doughnut-shaped structure. This unique interplay of phase and intensity in light with OAM opens up promising applications across diverse fields, ranging from quantum information in a high-dimensional structure [16] and communication in optics [17] to trapping optically [18] and the domain of tweezers that are optical [19].

In contrast to the connection of atoms ensembles with homogeneous lighting fields, an interaction with structured light may result in unexpectedly manifestations along with implications. These involve the development of entangled OAM states for the storage [20], the reduction of the spectra width [21], second harmonic synthesis [22], along with four-wave mixing (FWM) [23]. The structure of the light field is essential in these situations, promoting substantial attempts to develop patterned optical beams. According to a theoretical proposal, one method makes use of EIT for generating light with structure in confined atomic three- or four-level configuration [24–26]. Experimental confirmation of spatially structured transparency in a cold Rubidium atomic medium was achieved by Radwell et al. [27], utilizing a structural probe light beam. Another theoretically stated approach uses a tripod as well as coupled Λ arrangement to generate structured light [28]. Notably, the probing field is regarded as a vortex light in many reported methods, but the control fields lack OAM [29–33]. The choice that follows is taken in order to maintain the EIT condition because the diminishing core intensity of the control light beam causes the EIT behavior to be disturbed when it forms a vortex field. However, by adding a second control field to the vicinity of OAM, transparency may still be preserved [34].

Recent research has focused on OAM transferring via controlling beam to a probing beam. This can be accomplished by maintaining EIT characteristics in double-tripod setups through the inclusion of an additional non-vortex control field [35], as well as in atomic double-Λ systems along with quantum dot patterns in the shape of diamonds with four-wave mixing approach [36,37]. Experts investigated the efficiency of OAM transmission through weak probe fields, employing noise-induced coherence in V-type (Λ-type) configurations [38]. A method for efficiently transferring optical vortices has been examined by the researcher through inelastic two-wave mixing in an inverted-Y four-level atomic medium [39].

Intrigued by the potential of OAM to enhance control capabilities, we explore an innovative approach based on an atoms condensate controlled by vortices optical beams. Our focus extends to investigating how to create spatially structured spontaneous emission. Unlike previous work in Ref. [14], our scheme does not rely on the quantum interference of spontaneous emission. Instead, we introduce a microwave field to the upper level, creating a closed-loop atomic configuration. Quantum interference within this setup facilitates OAM transfer by both vortex fields to spontaneously emitting photons.

Diverging from conventional techniques such as probe absorption [24–26] and four-wave mixing methods [36,37,40] employed for OAM exchange and the generation of structured light, our proposed approach introduces a fresh and straightforward method through spontaneous emission measurement. The crux of our scheme lies in the creation of a spatially dependent spontaneous emission spectrum, wherein spontaneous emission is selectively suppressed in specific regions of azimuthal space, and concomitantly enhanced in others. This distinctive modulation offers valuable insights into the winding number (azimuthal quantum number) ℓ characterizing emerging patterned (structure) emitted light.

The subsequent sections of this paper unfold as follows: In Section 2, we elaborate on our proposed scheme and present the supporting equations, providing an expression for obtaining the spontaneously emitted spectrum. Section 3 delves into the investigation of our results under various conditions for the generated light. Finally, we draw conclusions and summarize our work in Section 4.

2. Theoretical model

Embarking on the exploration of spatially mapping spontaneous emission, our focus centers on a four-level atomic configuration distinguished by two lower states, $|b\rangle$ and $|c\rangle$, as well as two upper states, $|a_1\rangle$ and $|a_2\rangle$ (see Fig. 1). Adding intricacy to this setup, we introduce two optical vortices characterized by Rabi frequencies Ω_1 and Ω_2, steering distinct transitions: $|b\rangle \leftrightarrow |a_1\rangle$ and $|b\rangle \leftrightarrow |a_2\rangle$. This complex system extends to include excited states $|a_1\rangle$ and $|a_2\rangle$, intricately coupled with a microwave field Ω_μ to establish a closed-loop structure. The unfolding dynamics involve interactions with vacuum field modes, denoted as $E_{vacuum} = \sqrt{\frac{\hbar\omega_k}{\epsilon_0 V}}(b_k e^{i\nu_k t} - b_k^\dagger e^{-i\nu_k t})$, prompting the decay of upper levels $|a_1\rangle$ and $|a_2\rangle$ to the lower state $|c\rangle$. Capturing the essence of this intricate interplay, the interaction Hamiltonian within the dipole and Rotating-Wave Approximation (RWA) framework, driven by two OAM fields, is expressed as:

$$H_I = \hbar(\Omega_1|a_1\rangle\langle b| + \Omega_2|a_2\rangle\langle b| + \Omega_\mu|a_1\rangle\langle a_2|) + \hbar\sum_k (g_k^{(a_1)} e^{i(\omega_{a_1 c}-\nu_k)t}|a_1\rangle\langle c|b_k + g_k^{(a_2)} e^{i(\omega_{a_2 c}-\nu_k)t}|a_2\rangle\langle c|b_k) + h.c., \tag{1}$$

where the operators $b_k^\dagger$ and b_k correspond to the creation and annihilation operators of reservoir modes with frequency $\nu_k = ck$. The coupling constants $g_k^{(a_1)}(g_k^{(a_2)})$ represent the interaction strengths between the atomic dipoles $|a_1\rangle$ to $|c\rangle$ and $|a_2\rangle$ to $|c\rangle$, respectively. The resonant transition frequencies are denoted as $\omega_{a_1 c}$ and $\omega_{a_2 c}$ for the transitions involving $|a_1\rangle$ and $|a_2\rangle$ to $|c\rangle$, respectively, interacting with the corresponding reservoir modes. In the process of spontaneous decay, excited level atom eventually emits photons and transitions to a lower-energy state. The transition dynamics are determined by the interaction between the atom as well as the electromagnetic vacuum field. The interaction characteristic for the kth vacuum mode, represented as $g_k^{(a_1,a_2)}$, is determined by the equation $\sqrt{\frac{2\pi\nu_k}{V}}\hat{\epsilon_k}\cdot\mu_{nc}e^{-ikz_0}$. In this context, $\hat{\epsilon_k}$ denotes the electrically polarized vector corresponding to the released photon with frequency ν_k, $\mu_{nc} = \langle n|\mu|c\rangle$ (where $n = a_1, a_2$) signifies the transformation matrix element associated with the $|n\rangle \longleftrightarrow |c\rangle$ transition, V symbolizes the quantified volume, and z_0 indicates the precise location for the atom. In this dipole approximation, through which the atomic sizes are much less then the wavelength for light, the term e^{-ikz_0} is treated as a constant. Since optical vortices are carried by both controlling fields, the following definitions apply to the Rabi frequencies Ω_1 and Ω_2:

$$\Omega_1 = |\Omega_1| e^{i\ell_1\Phi}, \qquad \Omega_2 = |\Omega_2| e^{i\ell_2\Phi}, \tag{2}$$

with

$$|\Omega_1| = \epsilon_1(\frac{r}{w})^{|\ell_1|}e^{-\frac{r^2}{w^2}}, \qquad |\Omega_2| = \epsilon_2(\frac{r}{w})^{|\ell_2|}e^{-\frac{r^2}{w^2}}. \tag{3}$$

where the beam amplitudes are ϵ_1, ϵ_2, as well as the waist of the beam is w.

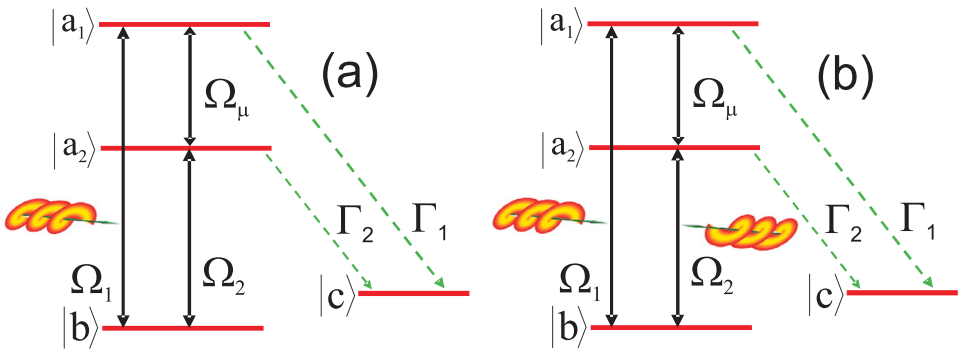

Fig. 1. (Color online) (a) Schematic representation of our proposal. (a) Depicts a four-level atom system driven by a single Laguerre–Gaussian (LG) mode control beam with an associated Rabi frequency Ω_1. (b) Illustrates the scenario where couple LG mode control beams Ω_1 and Ω_2 are applied, which manipulates atomic four-level system. Both degenerate excited states $|a_1\rangle$ and $|a_2\rangle$ are coupled with a microwave field Ω_μ. Subsequently, these excited states decay to a prevalent state $|c\rangle$ by spontaneously emitting a photon.

The comprehensive state description of a single atom interacting with its environment can be expressed

$$|\Psi(t)\rangle = A_{a_1,0_k}(t)|a_1,0_k\rangle + A_{a_2,0_k}(t)|a_2,0_k\rangle + A_{b,0_k}(t)|b,0_k\rangle + \sum_k A_{c,1_k}(t)|c,1_k\rangle, \tag{4}$$

where the probability amplitude $A_{j,0_k}(t)(j = a_1, a_2, b)$ represents the state of the atom at time t, $|0_k\rangle$ indicates that no photon has been emitted in the kth vacuum mode and, $A_{c,1_k}(t)$ represents the probability of the atom to be in the energy state $|c\rangle$ with $|1_k\rangle$ indicating one photon emitted in the kth vacuum mode. The suggested technique requires the detection of photons (with frequency ν_k) that spontaneously emit via both decay channels, $|a_1\rangle \to |c\rangle$ and $|a_2\rangle \to |c\rangle$, in order to quantify the light that is ultimately established. The photon's being identified, which provides information on the vacuum mode k and winding number $\ell_1(\ell_2)$ at any given time 't'. The equation of motion for the probability amplitudes can be obtained as follows through substitution of the previously mentioned function of waves for Schrödinger equation, which is governed by the Hamiltonian given in Eq. (1), and using the Weiskopf–Wigner approximation [41–46]

$$\begin{aligned}
\dot{A}_{b,0_k}(t) &= -i\Omega_1^* A_{a_1,0_k}(t) - i\Omega_2^* A_{a_2,0_k}(t),\\
\dot{A}_{a_1,0_k}(t) &= -i\Omega_1 A_{b,0_k}(t) - i\Omega_\mu A_{a_2,0_k}(t)\\
&\quad - \frac{\Gamma_1}{2}A_{a_1,0_k}(t) - \wp\frac{\sqrt{\Gamma_1\Gamma_2}}{2}A_{a_2,0_k}(t)e^{i\omega_{a_1a_2}t},\\
\dot{A}_{a_2,0_k}(t) &= -i\Omega_2 A_{b,0_k}(t) - i\Omega_\mu^* A_{a_1,0_k}(t)\\
&\quad - \frac{\Gamma_2}{2}A_{a_2,0_k}(t) - \wp\frac{\sqrt{\Gamma_1\Gamma_2}}{2}A_{a_1,0_k}(t)e^{-i\omega_{a_1a_2}t},\\
\dot{A}_{c,1_k}(t) &= -iA_{a_1,0_k}(t)g_k^{(a_1)}e^{i\delta_{k1}t} - iA_{a_2,0_k}(t)g_k^{(a_2)}e^{i\delta_{k2}t}.
\end{aligned} \tag{5}$$

In the above, $\wp = \frac{\vec{\mu}_{a_1,c}\cdot\vec{\mu}_{a_2,c}}{|\vec{\mu}_{a_1,c}||\vec{\mu}_{a_2,c}|}$ where $\vec{\mu}_{a_1,c}$ ($\vec{\mu}_{a_2,c}$) that expressed a matrix component associated with a transition $|a_1\rangle \to |c\rangle$ ($|a_2\rangle \to |c\rangle$). This interaction fundamentally represents quantum interference among the spontaneous decay pathways and is taken as zero. However, in our proposed scheme a closed-loop structure is established between two vortex pump fields and a microwave pump field applied to atomic transitions, leading to quantum interference phenomena in spontaneously emitted channels. This enables us to examine how the constituents that comprise the OAM-carrying vortex beam influencing the emitted spectrum.

The atom oscillates throughout short-time evolution between the excited states along with its ground state $|b\rangle$ in the presence of coherent driving. Nevertheless, because of spontaneous emission, the atom eventually decays to the state $|c\rangle$ in the long term. The ground state $|b\rangle$, the excited states $|a_1\rangle$ and $|a_2\rangle$, and their probability amplitudes, which all converge to zero as time approaches infinity, describe this decay as:

$$A_{c,1_k}(t\to\infty) = g_k^{(a_1)}\frac{M_1(\delta)}{N_1(\delta)} + g_k^{(a_2)}\frac{M_2(\delta)}{N_2(\delta)}. \tag{6}$$

where $\delta = \nu_k - \omega_{a_1c} + \frac{\omega_{a_1a_2}}{2}$, and

$$\begin{aligned}
M_1(\delta) &= A_{b,0_k}(0)[\Omega_1(\delta - \frac{\omega_{a_1a_2}}{2} + i\frac{\Gamma_1}{2}) + \Omega_2\Omega_\mu]\\
&\quad + A_{a_1,0_k}(0)[(\delta - \frac{\omega_{a_1a_2}}{2})(\delta - \frac{\omega_{a_1a_2}}{2} + i\frac{\Gamma_2}{2}) - |\Omega_2|^2]\\
&\quad + A_{a_2,0_k}(0)[(\delta - \frac{\omega_{12}}{2})\Omega_\mu + \Omega_1^*\Omega_2],
\end{aligned} \tag{7}$$

$$\begin{aligned}
M_2(\delta) &= A_{b,0_k}(0)[\Omega_1\Omega_\mu^* + \Omega_2(\delta + \frac{\omega_{a_1a_2}}{2} + i\frac{\Gamma_2}{2})]\\
&\quad + A_{a_1,0_k}(0)[(\delta + \frac{\omega_{12}}{2})\Omega_\mu^* + \Omega_1^*\Omega_2]\\
&\quad + A_{a_2,0_k}(0)[(\delta + \frac{\omega_{a_1a_2}}{2})\times(\delta + \frac{\omega_{a_1a_2}}{2} + i\frac{\Gamma_1}{2}) - |\Omega_1|^2],
\end{aligned} \tag{8}$$

$$\begin{aligned}
N_1(\delta) &= (\delta - \frac{\omega_{a_1a_2}}{2})(\delta - \frac{\omega_{a_1a_2}}{2} + i\frac{\Gamma_1}{2})(\delta - \frac{\omega_{a_1a_2}}{2} + i\frac{\Gamma_2}{2})\\
&\quad - |\Omega_1|^2(\delta - \frac{\omega_{a_1a_2}}{2} + i\frac{\Gamma_2}{2}) - |\Omega_2|^2(\delta - \frac{\omega_{a_1a_2}}{2} + i\frac{\Gamma_1}{2})\\
&\quad - (\delta - \frac{\omega_{12}}{2})|\Omega_\mu|^2 - (\Omega_1^*\Omega_2\Omega_\mu + \Omega_1\Omega_2^*\Omega_\mu^*),
\end{aligned} \tag{9}$$

$$\begin{aligned}
N_2(\delta) &= (\delta + \frac{\omega_{a_1a_2}}{2})(\delta + \frac{\omega_{a_1a_2}}{2} + i\frac{\Gamma_1}{2})(\delta + \frac{\omega_{a_1a_2}}{2} + i\frac{\Gamma_2}{2})\\
&\quad - |\Omega_1|^2(\delta + \frac{\omega_{a_1a_2}}{2} + i\frac{\Gamma_2}{2}) - |\Omega_2|^2(\delta + \frac{\omega_{a_1a_2}}{2} + i\frac{\Gamma_1}{2})\\
&\quad - (\delta + \frac{\omega_{12}}{2})|\Omega_\mu|^2 - (\Omega_1^*\Omega_2\Omega_\mu + \Omega_1\Omega_2^*\Omega_\mu^*).
\end{aligned} \tag{10}$$

By inserting the aforementioned coefficients from Eq. (4), the eventual state of the light-atom interaction mechanism in the long-time limit may be easily determined as $|\Psi(t\to\infty) = \sum_k A_{c,1_k}(t\to\infty)|c\rangle|1_k\rangle = |c\rangle|\gamma\rangle$ where

$$|\gamma\rangle = \sum_k A_{c,1_k}(t\to\infty)|1_k\rangle \tag{11}$$

represents the emitted photon state. Additionally, in our mathematical computations, we neglect influence of Doppler broadening (DB). The magneto-optical trap (MOT) is a widely used technique in such environments. To mitigate the impact of DB in investigations involving hot atomic mediums, a counter-propagating beam method may be used [47]. Notably, employing cold atoms is a straightforward strategy for addressing DB phenomena [48].

In our proposed scheme for detecting spatially structured spontaneous emitted photon interacting with a vortex beam and environmental modes, certain approximations have been made. Despite these approximations, the well-defined and engineered nature of light-atom interaction systems, their ability to exhibit quantum phenomena, and their extensive applications in various quantum technologies collectively justify classifying them as artificial quantum systems [49,50]. In the next part, we will go into more depth on the spontaneously emitted spectrum.

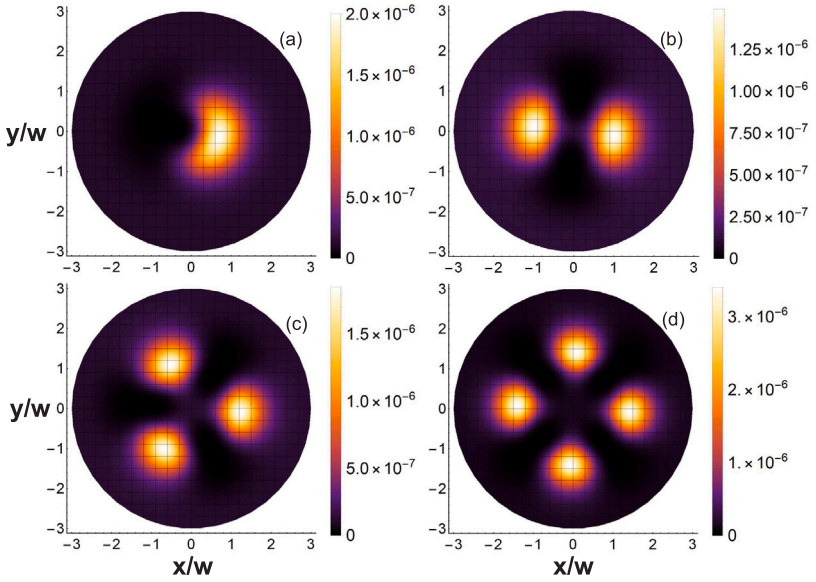

Fig. 2. (Color online) [a, b, c, d] Spatially dependent spontaneous emission profile for the case in which any one of the controlling beam is implemented as a vortex beam, with the atom initially in the ground state i.e. $A_{b,0_k} = 1$, $A_{a_1,0_k}(0) = 0$, and $A_{a_2,0_k}(0) = 0$. Here panels (a), (b), (c), and (d) correspond to different values of ℓ_1: $\ell_1 = 1$, $\ell_1 = 2$, $\ell_1 = 3$, and $\ell_1 = 4$, respectively. The selected parameters are fixed at $\delta = 0$, $\omega_{a_1a_2} = 10\Gamma$, $\epsilon_1 = 1\Gamma$, $g_k^{(a_1)} = g_k^{(a_2)} = 1\Gamma$, $\Omega_2 = 0.5\Gamma$, $\Omega_\mu = 0.5\Gamma$, $\Gamma_1 = 1\Gamma$, $\Gamma_2 = 1\Gamma$ and $\Gamma = 1$ MHz.

3. Azimuthally dependent spontaneous emission

In the following section, we delve into the intricacies of the emission spectrum, shedding light on the fascinating process of transferring the optical vortex from control fields to the spontaneous emission spectra. Moreover, we embark on an exploration of the spatial configuration's tunability within the spectra by manipulating the driving fields. The mathematical expression for the spontaneously emitted spectrum is articulated as follows [14]:

$$S = |A_{c,1_k}(t \to \infty)|^2, \tag{12}$$

where $A_{c,1_k}(t \to \infty)$ is given in Eq. (6).

By incorporating Eqs. (6)–(10) into the above equation, an interference term $\Omega = \Omega_1\Omega_2^*\Omega_\mu^*$ emerges in the emission spectrum, playing a crucial role in transferring OAM characteristics to generated emitted spectrum. The pumped fields possess finite OAM, as shown in Eqs. (2) and (3). Consequently, the interference expression may be articulated as follows:

$$\Omega = |\Omega_1|\,|\Omega_2|\,\Omega_\mu^* e^{i(\ell_1-\ell_2)\Phi}. \tag{13}$$

Figs. 2–6 illustrate diverse instances of spatially structured spontaneous emission, as characterized by the equation presented in Eq. (12). The utilization of inhomogeneous vortex beams introduces a spatial dependency in the atom-light interaction. Consequently, the spontaneously emitted photon encapsulates information pertaining to the atom's position within the azimuthal plane, leading to the precise localization of the atom at the point of photon detection.

In Fig. 2, we present spatially varying spontaneous emission profiles corresponding to scenarios where one of the driving fields Ω_1 carries OAM as shown in Fig. 1(a). Specifically, panels (a) through (d) depict cases with $\ell_1 = 1$, $\ell_1 = 2$, $\ell_1 = 3$, and $\ell_1 = 4$, respectively. Assuming the atom starts in the ground state $|b\rangle$, we analyze the intensity distribution with initial conditions $A_{b,0_k} = 1$, $A_{a_1,0_k}(0) = 0$, and $A_{a_2,0_k}(0) = 0$. The relationship between the coupling constants of the atom as well as the reservoir mode are given by $g_k^{(a_1)} = g_k^{(a_2)} = 1\Gamma$, pumping vortex field amplitudes $\epsilon_1 = 1\Gamma$, microwave field $\Omega_\mu = 0.5\gamma$, nonvortex field $\Omega_2 = 0.5\gamma$, energy separation of the higher levels $\omega_{a_1a_2} = 10\Gamma$, spontaneous decay rates $\Gamma_1 = \Gamma_2 = \Gamma$, along with detuning $\delta = 0$ with $\Gamma = 1$ MHz.

As can be seen in Fig. 2(a–d), the spatial dependence of the emitted light profile reveals petal-like structures. The yellowish brilliant region inside each petal indicates the greatest amount of spontaneous emission, emphasizing the atom's precise localization at that location. The dark areas indicate the suppression of spontaneous emission. Simultaneously, the orange and purple spatial areas demonstrate a modest degree of spontaneous emission in contrast to the yellowish magnificent area. Upon closer examination, we observe that as the OAM number is increased, the number of petal patterns in the emitted structure increases. Specifically, Fig. 2(d) demonstrates spontaneous emission occurring in four distinct regions for $\ell_1 = 4$. This shows that structured spontaneous emission spectra may be generated through applying an OAM-carrying optical field to a atomic four-level system. This would transmit the control field Ω_1's vorticity to the spontaneously emitted photons.

In Fig. 3(a–d), we delve into the exploration of position-dependent spontaneous emission profiles while systematically decreasing the strength of the non-vortex pump field from $\Omega_2 = 0.5\Gamma$ to $\Omega_2 = 0.1\Gamma$. In alignment with the case in Fig. 2, we maintain the configuration of having one of the control fields carrying OAM, with specific cases illustrated as (a) $\ell_1 = 1$, (b) $\ell_1 = 2$, (c) $\ell_1 = 3$, and (d) $\ell_1 = 4$. The characteristics beyond the pump field strength are similar with those discussed throughout the previous discussion (Fig. 2). After comparing the emission spectra's spatial patterns, a striking observation emerges: the strength of the non-vortex pump field emerges as a key determinant in shaping the spectral-spatial characteristics of maximum spontaneous emission. The systematic decrease from $\Omega_2 = 0.5\gamma$ to $\Omega_2 = 0.1\Gamma$ exerts a discernible influence on the emission spectra, allowing for a controlled modulation of the spatial distribution of spontaneous emission. Crucially, the incorporation of OAM in the control field introduces an additional layer of control over the spectral-spatial shape of maximum spontaneous emission. As evidenced in Fig. 3(a–d), different OAM values lead to distinct patterns in the position-dependent spontaneous emission profiles. This observation underscores the nuanced interplay between the OAM-carrying control field and the resultant emission spectra.

Fig. 4 presents a series of instances demonstrating the spatial dependence of spontaneously emitted light when both driving fields carry OAM. The insets (a–d) show the spatially distributed portions of the spontaneous emission spectrum S at various OAM valuers, specifically (a) $\ell_1 = \ell_2 = 1$, (b) $\ell_1 = \ell_2 = 2$, (c) $\ell_1 = \ell_2 = 3$, and (d) $\ell_1 = \ell_2 = 4$. As previously stated, we assume the atom is first formed in

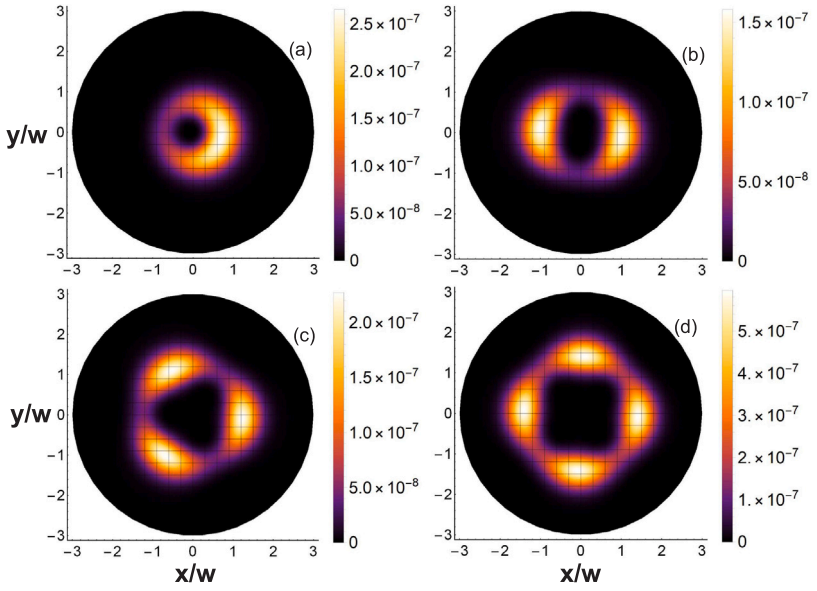

Fig. 3. (Color online) [a, b, c, d] Spatially dependent spontaneous emission profile for the case in which any one of the controlling beam is implemented as a vortex beam, with the atom initially in the ground state i.e. $A_{b,0_k} = 1$, $A_{a_1,0_k}(0) = 0$, and $A_{a_2,0_k}(0) = 0$. Panels (a), (b), (c), and (d) correspond to different values of ℓ_1: $\ell_1 = 1$, $\ell_1 = 2$, $\ell_1 = 3$, and $\ell_1 = 4$, respectively. Here, $\Omega_2 = 0.1\Gamma$ with all other parameters held constant as in Fig. 2.

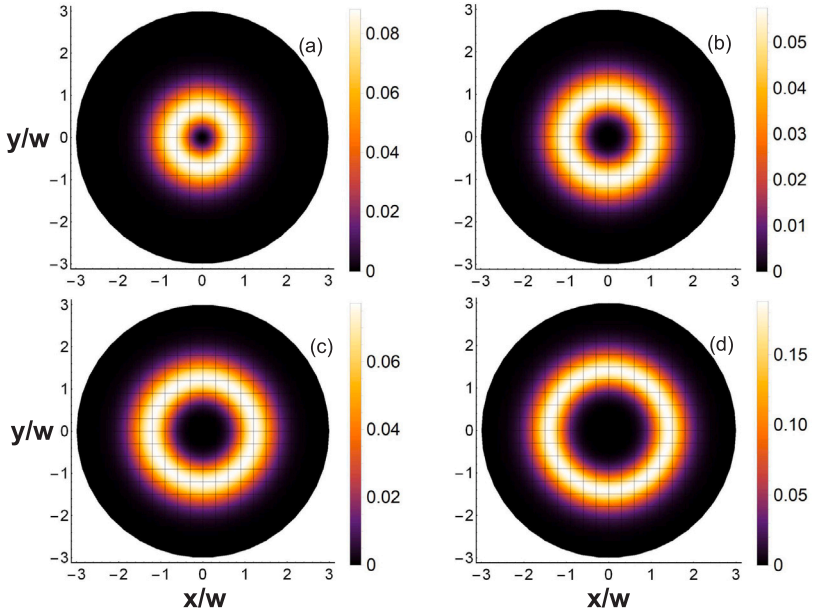

Fig. 4. (Color online) [(a), (b), (c), (d)] Spatially dependent spontaneous emission profile for a situation wherein each control beams are implemented as vortex lights, with the atom initially in the ground state i.e. $A_{b,0_k} = 1$, $A_{a_1,0_k}(0) = 0$, and $A_{a_2,0_k}(0) = 0$. Panels (a), (b), (c), and (d) correspond to different values of $\ell_1(\ell_2)$: $\ell_1 = \ell_2 = 1$, $\ell_1 = \ell_2 = 2$, $\ell_1 = \ell_2 = 3$, and $\ell_1 = \ell_2 = 4$, respectively. Here, $\epsilon_1 = \epsilon_2 = \Gamma$, with all other parameters held constant as in Fig. 2.

the ground position $|b\rangle$. $\epsilon_1 = \epsilon_2 = \Gamma$ is the set of vortex field pumping amplitudes, the remaining variables are kept as they are in Fig. 2. Examining Fig. 4(a–d), a distinct ring-shaped pattern in the spectral-spatial distribution of spontaneous emission becomes evident, akin to a vortex beam. Notably, as the OAM of the control field increases, the size of the vanishing center expands. This observed behavior aligns with the characteristic features of a standard LG mode. The ring-shaped spatial distribution in Fig. 4(a–d) underscores the influence of OAM on the emitted light, leading to a structured emission spectrum reminiscent of vortex beams. This shows that driving fields having OAM may be adjusted and tuned to modify the spatial properties of spontaneous emission.

Next, we will explore cases beyond symmetric helicity and show that beams formed in this method can take many forms. This is shown by looking at a case where the vortex control beams have distinct OAM values. Fig. 5 shows that when vortex control beams have different OAM values, the spontaneous emission spectrum S varies significantly, unlike the previous discussion which had same vorticity controlling beam. At $\ell_1 = 1$ and $\ell_2 = 3$, the spectral-spatial emission spectrum is shown in Fig. 5(a). The normal ℓ–fold symmetry shown in Fig. 4 is clearly broken, and a more complex pattern with more singularities is seen. A rotational symmetry of $|\ell_1 - \ell_2|$ – is followed by this disruption. See Fig. 5(a) for an illustration of the resultant emission profile, which is similar to a composite structured beam with a central charge of +1 and two surrounding charge vortices of +1 [51]. Fig. 5(b–d) shows

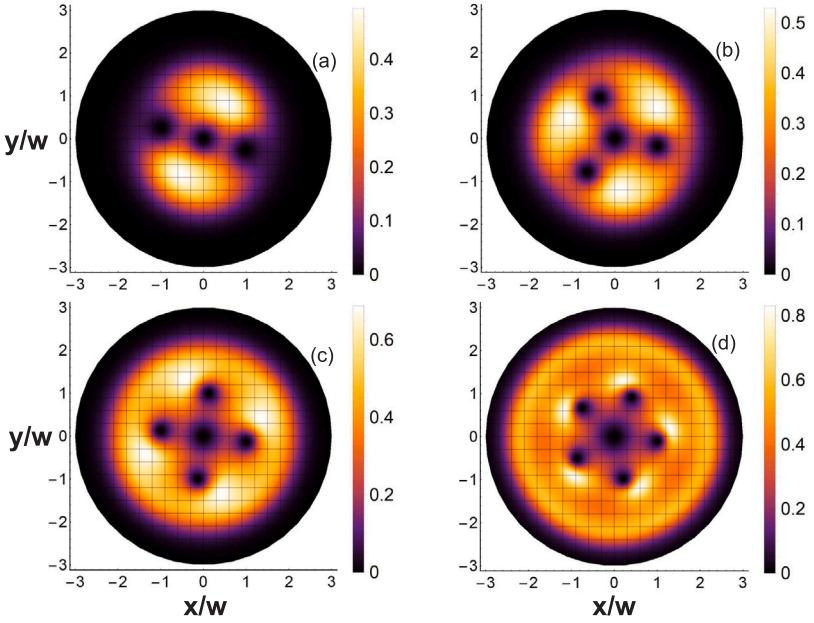

Fig. 5. (Color online) [(a), (b), (c), (d)] Spatially dependent spontaneous emission profile for a situation wherein each control beams are implemented as vortex lights, with the atom initially in the ground state i.e. $A_{b,0_k} = 1$, $A_{a_1,0_k}(0) = 0$, and $A_{a_2,0_k}(0) = 0$. Panels (a), (b), (c), and (d) correspond to cases such that $\ell_1 < \ell_2$ i.e. (a) $\ell_1 = 1, \ell_2 = 3$, (b) $\ell_1 = 1, \ell_2 = 4$, and (c) $\ell_1 = 1, \ell_2 = 5$, (d) $\ell_1 = 1, \ell_2 = 6$. Here, $\epsilon_1 = \epsilon_2 = 1$, $\delta = 0.48\Gamma$, with all other parameters held constant as in Fig. 2.

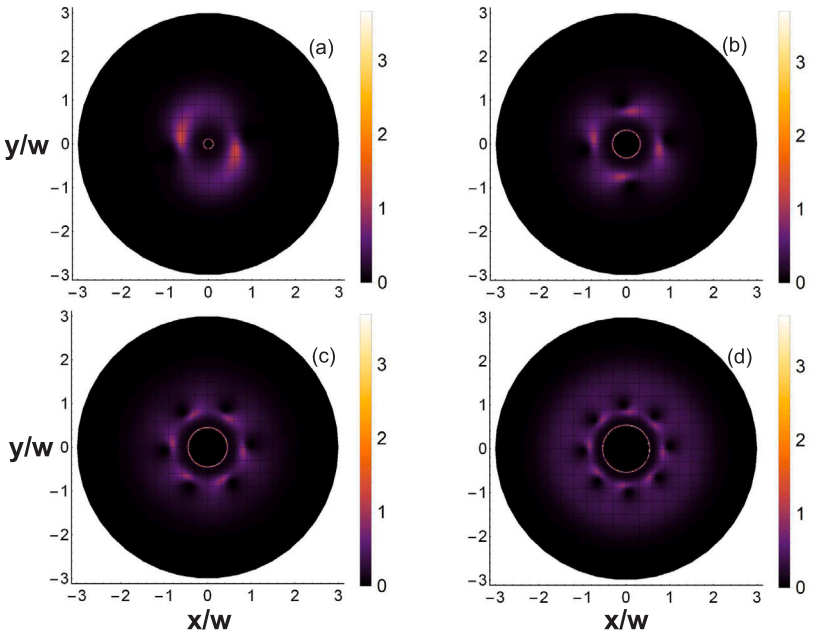

Fig. 6. (Color online) [a–d]Spatially dependent spontaneous emission profile for a situation wherein each control beams are implemented as vortex lights, with the atom initially in the ground state i.e. $A_{b,0_k} = 1$, $A_{a_1,0_k}(0) = 0$, and $A_{a_2,0_k}(0) = 0$. Panels (a), (b), (c), and (d) correspond to different values of (a) $\ell_1 = -\ell_2 = 1$, (b) $\ell_1 = -\ell_2 = 2$, (c) $\ell_1 = -\ell_2 = 3$, and (d) $\ell_1 = -\ell_2 = 4$, and the remaining parameters being the same as Fig. 5.

similar patterns in other scenarios as well, when $\ell_1 = 1$ is fixed and ℓ_2 is adjusted from 4 to 6.

We now investigate the scenario in which the beams exhibit opposite vorticities, specifically when $\ell_1 = -\ell_2 = \ell$. Figs. 6(a–d) illustrate the spatially dependent spontaneous emission profiles for different values of ℓ, namely (a) $\ell_1 = -\ell_2 = 1$, (b) $\ell_1 = -\ell_2 = 2$, (c) $\ell_1 = -\ell_2 = 3$, and (d) $\ell_1 = -\ell_2 = 4$. The parameters considered are $\epsilon_1 = 1\Gamma$, $\epsilon_2 = 1\Gamma$, and, as in the previous cases, the atoms are assumed to be initially prepared in the ground state, with $A_{b,0_k} = 1$, $A_{a_1,0_k}(0) = 0$, and $A_{a_2,0_k}(0) = 0$. Other parameters include $\delta = 4.08\Gamma$ (where spontaneous emission reaches its maximum), $g_k^{(1)} = g_k^{(2)} = 1\Gamma$, $\omega_{12} = 10\Gamma$, $\Omega_\mu = 0.5\Gamma$, and $\Gamma_1 = \Gamma_2 = 1\Gamma$ with $\Gamma = 1$ MHz. As depicted in Fig. 6, the spatially dependent spontaneous emission exhibits a distinctive structure characterized by azimuthal dependence governed by $|\Omega_1||\Omega_2||\Omega_\mu|\cos(\ell\phi)$. Figs. 6(a–d) reveal the formation of a dark Ferris wheel structure [52,53] with a $2\ell-$fold symmetry, clearly demonstrating spectral-spatial spots where the spontaneous emission is suppressed.

Our approach to achieving spatially varying spontaneous emission presents a novel and straightforward solution. By manipulating key parameters like light-atom detuning, the strength of LG beams, and the

initial state of the atoms, we can achieve highly tunable spontaneous emission spectra.

3.1. Discussion

In our study, we analyze the spontaneously emitted structured light spectrum in this setup. Specifically, we introduce a microwave field to the upper level, creating a closed-loop atomic configuration. In short-time evolution, the atom may remain in the ground state $|b\rangle$ while oscillating between the excited states $|a_1\rangle$ ($|a_2\rangle$). However, in the long-time limit, it will decay to the state $|c\rangle$ as a result of spontaneous emission. The quantum interference arising from this closed-loop configuration facilitates the transfer of OAM from the driving vortex fields to the spontaneously emitted photons, resulting in spatially dependent spontaneous emission profiles.

In order to explain in more detail how OAM is transferred from the vortex fields to the spontaneously emitted photons in our proposed scheme, we highlight the critical role of the microwave field in establishing quantum interference between the two upper degenerate levels. Specifically, in the absence of the microwave field connecting these upper states, and when the atom is initially prepared in the ground state $|b\rangle$, the quantum interference term in Eq. (12) vanishes. As a result, the transfer of OAM from the driving vortex fields to the emitted spontaneous emission spectrum is inhibited.

In such a scenario, where the closed-loop structure formed by the microwave field is absent, the spontaneously emitted spectrum becomes spatially uniform, showing no azimuthal dependence. This is in stark contrast to the case where the microwave field is present and quantum interference is active, leading to a structured emission spectrum that varies with the OAM number of the optical vortices. This demonstrates that the microwave field is essential in enabling the transfer of OAM characteristics from the vortex beams to the spontaneously emitted photons.

4. Conclusion

In summary, this paper delved into the phenomenon of spontaneously generated structured light within an atomic system. By examining a four-level atom subjected to the influence of two vortex beams and a microwave field acting on the upper two levels, we illustrated OAM transfer from the pump fields to the spontaneously emitted light spectra. Furthermore, the interference of driving two fields as well as microwave field, along with their spatially dependent intensity and phase distribution, led to the emergence of diverse spatial profiles in the emitted light, surpassing the conventional OAM mode. Importantly, the tunability of these spatial profiles was demonstrated through precise control of the phase or OAM of the driving fields. This could facilitate the creation of spatially structured spectra, where spontaneous emission is quenched in certain areas of azimuthal space while being enhanced in others. This presents an intriguing technique for manipulating the configuration for optical fields, potentially beneficial in structured light research, such as trapping or rotating particles using superradiant structured light and in the fabrication of OAM lasers [54,55]. In most cases, significant pumpings are required for the superradiance to occur. In our suggested technique, this is accomplished by using an optical cavity or high-intensity structured beams to excite the electrons to higher levels. This method may be used for creating and enhancing structured light in a coherent way. Achieving the desired outcome of distinct profiles in structured light may be facilitated by accurately controlling both the excitation process and the atomic properties. Furthermore, our idea of vortex pumping to manipulate the atomic spontaneously spectra offers a possible way to improve magnetometers and other precision measurement techniques.

CRediT authorship contribution statement

Muqaddar Abbas: Writing – review & editing, Writing – original draft, Methodology, Formal analysis, Data curation, Conceptualization. **Seyyed Hossein Asadpour:** Formal analysis, Data curation, Conceptualization. **Rahmatullah:** Conceptualization, Formal analysis, Investigation, Visualization, Writing – review & editing. **Feiran Wang:** Conceptualization, Formal analysis, Investigation. **Hamid R. Hamedi:** Writing – review & editing, Writing – original draft, Funding acquisition, Formal analysis, Data curation, Conceptualization. **Pei Zhang:** Visualization, Validation, Supervision, Funding acquisition, Formal analysis, Data curation.

Declaration of competing interest

The authors declare that they have no known competing financial interests or personal relationships that could have appeared to influence the work reported in this paper.

Acknowledgments

This work was supported by the National Nature Science Foundation of China grant no. 12174301, the Natural Science Basic Research Program of Shaanxi, China grant no. 2023-JC-JQ-01, and the Open Fund of State Key Laboratory of Acoustics grant no. SKLA202312.

Data availability

Data will be made available on request.

References

[1] Scully MO, Zubairy MS. Quantum Optics. England: Cambridge University Press; 1997.
[2] Zhu S-Y, Scully MO. Spectral line elimination and spontaneous emission cancellation via quantum interference. Phys Rev Lett 1996;76:388.
[3] Ghafoor F, Zhu SY, Zubairy MS. Amplitude and phase control of spontaneous emission. Phys Rev A 2000;62:013811.
[4] Li JH. Control of spontaneous emission spectra via an external coherent magnetic field in a cycle-configuration atomic medium. Eur Phys J D 2007;42:467.
[5] Scully MO, Zhu S-Y, Gavrielides A. Degenerate quantum-beat laser: Lasing without inversion and inversion without lasing. Phys Rev Lett 1989;62:2813.
[6] Harris SE, Field JE, Imamoğlu A. Nonlinear optical processes using electromagnetically induced transparency. Phys Rev Lett 1990;64:1107.
[7] Scully MO. Correlated spontaneous-emission lasers: Quenching of quantum fluctuations in the relative phase angle. Phys Rev Lett 1975;55:2802.
[8] Scully MO. Enhancement of the index of refraction via quantum coherence. Phys Rev Lett 1991;67:1855.
[9] Zhou P, Swain S. Absorption spectrum and gain without inversion of a driven two-level atom with arbitrary probe intensity in a squeezed vacuum. Phys Rev A 1997;55:772.
[10] Garraway BM, Knight PL. Cavity modified quantum beats. Phys Rev A 1996;54:3592.
[11] Zhu S-Y, Chen H, Huang H. Quantum interference effects in spontaneous emission from an atom embedded in a photonic band gap structure. Phys Rev Lett 1997;79:205.
[12] Berman P. Analysis of dynamical suppression of spontaneous emission. Phys Rev A 1998;58:4886.
[13] li Li Fu, Zhu Shi-Yao. Resonance fluorescence quenching and spectral line narrowing via quantum interference in a four-level atom driven by two coherent fields. Phys Rev A 1999;59:2330.
[14] Paspalakis E, Knight PL. Phase control of spontaneous emission. Phys Rev Lett 1998;81:293.
[15] Allen L, Beijersbergen MW, Spreeuw RJC, Woerdman JP. Orbital angular momentum of light and the transformation of Laguerre-Gaussian laser modes. Phys Rev A 1992;45:8185.
[16] Dada AC, Leach J, Buller GS, Padgett MJ, Andersson E. Experimental high-dimensional two-photon entanglement and violations of generalized Bell inequalities. Nat Phys 2011;7:677.
[17] Wang J, Yang J-Y, Fazal IM, Ahmed N, Yan Y, Huang H, et al. Terabit free-space data transmission employing orbital angular momentum multiplexing. Nat Photonics 2012;6:488.

[18] Garcés-Chávez V, McGloin D, Padgett MJ, Dultz W, Schmitzer H, Dholakia K. Observation of the transfer of the local angular momentum density of a multiringed light beam to an optically trapped particle. Phys Rev Lett 2003;91:093602.
[19] Padgett MJ, Bowman R. Tweezers with a twist. Nat Photonics 2011;5:343.
[20] Ding DS, Zhang W, Zhou ZY, Shi S, Xiang G-Y, Wang X-S, et al. Quantum storage of orbital angular momentum entanglement in an atomic ensemble. Phys Rev Lett 2015;114:050502.
[21] Chanu SR, Natarajan V. Narrowing of resonances in electromagnetically induced transparency and absorption using a Laguerre-Gaussian control beam. Opt Commun 2013;295:150.
[22] Dholakia K, Simpson NB, Padgett MJ, Allen L. Second-harmonic generation and the orbital angular momentum of light. Phys Rev A 1996;54:R3742.
[23] Walker G, Arnold AS, Franke-Arnold S. Trans-spectral orbital angular momentum transfer via four-wave mixing in Rb vapor. Phys Rev Lett 2012;108:243601.
[24] Han L, Cao M, Liu R, Liu H, Guo W, Wei D, et al. Identifying the orbital angular momentum of light based on atomic ensembles. Eur Phys Lett 2012;99:34003.
[25] Sharma S, Dey TN. Phase-induced transparency-mediated structured-beam generation in a closed-loop tripod configuration. Phys Rev A 2017;96:033811.
[26] Shujaat A, Saleem U, Abbas M, Rahmatullah. Azimuthal modulation of probe absorption and transfer of optical vortices. Phys Scr 2020;95:085106.
[27] Radwell N, Clark TW, Piccirillo B, Barnett SM, Franke-Arnold S. Spatially dependent electromagnetically induced transparency. Phys Rev Lett 2015;114:123603.
[28] Hamedi HR, Kudriašov V, Ruseckas J, Juzeliūnas G. Azimuthal modulation of electromagnetically induced transparency using structured light. Opt Express 2018;26:28249.
[29] Dutton Z, Ruostekoski J. Transfer and storage of vortex states in light and matter waves. Phys Rev Lett 2004;93:193602.
[30] Pugatch R, Shuker M, Firstenberg O, Ron A, Davidson N. Topological stability of stored optical vortices. Phys Rev Lett 2007;98:203601.
[31] Wang T, Zhao L, Jiang L, Yelin SF. Diffusion-induced decoherence of stored optical vortices. Phys Rev A 2008;77:043815.
[32] Xie X-T, Li W-B, Yang X. Bright, dark, bistable bright, and vortex spatial-optical solitons in a cold three-state medium. J Opt Soc Am B 2006;23:1609.
[33] Moretti D, Felinto D, Tabosa JWR. Collapses and revivals of stored orbital angular momentum of light in a cold-atom ensemble. Phys Rev A 2009;79:023825.
[34] Ruseckas J, Mekys A, Juzeliūnas G. Slow polaritons with orbital angular momentum in atomic gases. Phys Rev A 2011;83:023812.
[35] Ruseckas J, Kudriašov V, Yu IA, Juzeliūnas G. Transfer of orbital angular momentum of light using two-component slow light. Phys Rev A 2013;87:053840.
[36] Hamedi HR, Ruseckas J, Juzeliūnas G. Exchange of optical vortices using an electromagnetically-induced-transparency–based four-wave-mixing setup. Phys Rev A 2018;98:013840.
[37] Rahmatullah, Abbas M, Ziauddin, Qamar S. Spatially structured transparency and transfer of optical vortices via four-wave mixing in a quantum-dot nanostructure. Phys Rev A 2020;101:023821.
[38] Asadpour SH, Ziauddin, Abbas Muqaddar, Hamedi HR. Exchange of orbital angular momentum of light via noise-induced coherence. Phys Rev A 2022;105:033709.
[39] Deng X, Shui T, Yang A-X. Inelastic two-wave mixing induced high-efficiency transfer of optical vortices. Opt Express 2024;32:16611.
[40] Meng C, Shui T, Yang W-X. Coherent transfer of optical vortices via backward four-wave mixing in a double-Λ atomic system. Phys Rev A 2023;107:053712.
[41] Lambropoulos P, Nikolopoulos GM, Neilsen TR, Bay S. Fundamental quantum optics in structured reservoirs. Rep Prog Phys 2000;63:455.
[42] Lodahl P, van Driel AF, Nikolaev IS, Irman A, Overgaag K, Vanmaekelbergh D, et al. Controlling the dynamics of spontaneous emission from quantum dots by photonic crystals. Nature 2004;430:654.
[43] Noda S, Fujita M, Asano T. Spontaneous-emission control by photonic crystals and nanocavities. Nat Photonics 2007;1:449.
[44] Pelton M. Modified spontaneous emission in nanophotonic structures. Nat Photonics 2015;9:427.
[45] Goetz RE, Bartschat K. Quantum control of entangled photon-pair generation in electron-atom collisions driven by laser-synthesized free-electron wave packets. Phys Rev A 2021;103:043112.
[46] Asadpour SH, Kirova Te, Hamedi HR, Yannopapas Va, Paspalakis E. Azimuthal dependence of electromagnetically induced grating in a double V-type atomic system near a plasmonic nanostructure. Eur Phys Jr Plus 2023;138:246.
[47] Ye CY, Zibrov AS, Rostovtsev YV, Scully MO. Unexpected Doppler-free resonance in generalized double dark states. Phys Rev A 2002;65:043805.
[48] Uhlenberg G, Dirscherl J, Walther H. Magneto-optical trapping of silver atoms. Phys Rev Lett 2000;62:063404.
[49] Joo J, Bourassa J, Blais A, Sanders BC. Electromagnetically induced transparency with amplification in superconducting circuits. Phys Rev Lett 2010;104:193601140.
[50] Longo P, Keitel CH, Evers J. Tailoring superradiance to design artificial quantum systems. Sci Rep 2016;6:23628.
[51] Hamedi HR, Ruseckas J, Paspalakis E, Juzeliūnas G. Transfer of optical vortices in coherently prepared media. Phys Rev A 2019;99:033812.
[52] F.-Arnold S, Leach J, Padgett MJ, Lembessis VE, Ellinas D, Wright AJ, et al. Optical ferris wheel for ultracold atoms. Opt Express 2007;15:8619.
[53] Hamedi HR, Kudriašov V, Jia Ning, Qian Jing, Juzeliūnas Gediminas. Ferris wheel patterning of rydberg atoms using electromagnetically induced transparency with optical vortex fields. Opt Lett 2021;46:4204.
[54] Hotter Christoph, Plankensteiner David, Ostermann Laurin, Ritsch Helmt. Superradiant cooling, trapping, and lasing of dipole-interacting clock atoms. Opt Express 2019;27:31193.
[55] Gold D, Huft P, Young C, Safari A, Walker T, Saffman M, et al. Spatial coherence of light in collective spontaneous emission. PRX Quantum 2022;3:010338.